


# Glenoid Concavity Affects Anterior Shoulder Stability in an Active-Assisted Biomechanical Model

Sebastian Oenning,<sup>\*†</sup> MD , Jens Wermers,<sup>‡</sup> Prof, MSc, Stefanie Taenzler,<sup>†</sup> BSc, Philipp A. Michel,<sup>†</sup> MD, Michael J. Raschke,<sup>†</sup> Prof, MD, and J. Christoph Katthagen,<sup>†</sup> Prof, MD  
Investigation performed at the Department of Trauma, Hand and Reconstructive Surgery, University Hospital Muenster, Muenster, Germany

**Background:** The treatment of bony glenoid defects after anteroinferior shoulder dislocation currently depends on the amount of glenoid bone loss (GBL). Recent studies have described the glenoid concavity as an essential factor for glenohumeral stability. The role of glenoid concavity in the presence of soft tissue and muscle forces is still unknown.

**Hypothesis:** Glenoid concavity would have a major impact on glenohumeral stability in an active-assisted biomechanical model including soft tissue and the rotator cuff's compression forces.

**Study Design:** Controlled laboratory study.

**Methods:** In 8 human shoulder specimens, individual coordinate systems were calculated based on anatomic landmarks. The glenoid concavity was measured biomechanically and based on computed tomography. Static load was applied to the rotator cuff tendons and the deltoid muscle. In a robotic test setup, anteriorly directed force was applied to the humeral head until translation of 5 mm ( $N_{ant}$ ) was achieved.  $N_{ant}$  was used as a parameter indicating shoulder stability. This was performed in the following testing stages: (1) intact joint, (2) labral lesion, (3) 10% GBL, and (4) 20% GBL. The 8 specimens were divided equally into 2 subgroups (low concavity [LC] versus high concavity [HC]), with 4 specimens each, according to the previously measured concavity.

**Results:** Anterior glenohumeral stability was highly correlated with the native glenoid concavity ( $R^2 = 0.8$ ). In the testing stages 1 to 3, we found a significantly higher mean stability in the HC subgroup compared with the LC subgroup ( $P \leq .0142$ ). The HC subgroup still showed higher absolute  $N_{ant}$  values with 20% GBL; however, there was no significant difference from the LC subgroup. The loss of stability in 20% GBL was correlated with the initial concavity ( $R^2 = 0.86$ ). Thus, a higher loss of  $N_{ant}$  in the HC subgroup was observed ( $P = .0049$ ).

**Conclusion:** In an active-assisted model with intact soft tissue surrounding and muscular compression forces, the glenoid concavity correlates with shoulder stability. In bony defects, loss of concavity is an essential factor causing instability. Due to their significantly higher native stability, glenoids with HC can tolerate a higher amount of GBL.

**Clinical Relevance:** Glenoid concavity should be considered in an individualized treatment of bony glenoid defects. Further studies are required to establish reference values and develop therapeutic algorithms.

**Keywords:** Bankart lesion; bony shoulder stability ratio; glenoid bone loss; glenoid concavity; instability; shoulder

Due to the glenohumeral anatomy, the shoulder joint provides the highest range of motion of all human joints.<sup>17</sup> The excessive mobility predisposes the glenohumeral joint to instability, leading to mainly anteroinferior humeral dislocation. Concomitantly, glenoid injuries include not only labral lesions (Bankart lesions) or glenolabral articular

disruption but also glenoid fractures, occurring in up to 40% to 50% of patients after first-time anteroinferior dislocation.<sup>2-4,6,19</sup>

The principle of concavity compression describes the interaction between the concave glenoid, shaped by the glenoid bone stock, articular cartilage, and the labrum, and the glenohumeral compression forces exerted by the rotator cuff.<sup>7,14,15,19</sup> Especially in midrange glenohumeral motion, stability is dependent mainly on concavity compression, due to maximum capsular and ligamentous

The Orthopaedic Journal of Sports Medicine, 12(6), 23259671241253836  
DOI: 10.1177/23259671241253836  
© The Author(s) 2024

This open-access article is published and distributed under the Creative Commons Attribution - NonCommercial - No Derivatives License (<https://creativecommons.org/licenses/by-nc-nd/4.0/>), which permits the noncommercial use, distribution, and reproduction of the article in any medium, provided the original author and source are credited. You may not alter, transform, or build upon this article without the permission of the Author(s). For article reuse guidelines, please visit SAGE's website at <http://www.sagepub.com/journals-permissions>.

laxity.<sup>15,17,19,23,27,28</sup> In a cadaveric study, Wermers et al<sup>26</sup> found the highest glenoid concavity in anteroinferior, posteroinferior, and superior positions.

In the case of glenoid bone loss (GBL), threshold values indicating bony reconstruction have decreased in the last decade. Studies have shown an increase of instability with GBL between 13.5% and 16%.<sup>3,12,21,22</sup> In addition, the loss of glenoid concavity plays a major role in glenohumeral instability. Focusing on the 3-dimensional (3D) glenoid morphology as a main glenohumeral stabilizer, Moroder et al<sup>19</sup> established the computed tomography (CT)-based bony shoulder stability ratio (BSSR), depending on the glenoid depth and the radius of the humeral head. By performing CT-based finite element analyses, a high correlation between glenoid concavity and shoulder stability was found.<sup>18</sup> Biomechanically, Wermers et al<sup>27</sup> confirmed the importance of the glenoid concavity in cadaveric glenoids, describing a significant reduction of anterior stability in the presence of anterior GBL. Physiological stabilizing forces exerted by the rotator cuff were not included in this osteochondral model.

Anterior glenohumeral stability and the impact of the glenoid concavity have yet to be investigated in an active-assisted model including the rotator cuff's compression force. We hypothesized that glenoid concavity would play an integral role for glenohumeral stability in the presence of intact soft tissue surrounding and the mechanism of concavity compression. Therefore, we developed a biomechanical model based on the physiological distribution of forces exerted by the rotator cuff and the deltoid muscle.<sup>7,25,31</sup>

## METHODS

### Specimen Preparation

A total of 8 fresh-frozen human cadaveric shoulders (3 right, 5 left; 1 female shoulder, 7 male shoulders; mean age,  $82.25 \pm 8.12$  years [age range, 76-98 years]) with intact rotator cuff on magnetic resonance imaging scans were included with institutional review board approval (IRB No. 2022-323-f-S, University of Muenster, Germany). All donors provided written consent to use their bodies for scientific and/or educational purposes. After thawing of the specimens at room temperature, preparation included skin and subcutaneous tissue resection. The deltoid muscle, all rotator cuff tendons, the biceps brachii muscle, the joint capsule, the glenohumeral ligaments, and the labrum

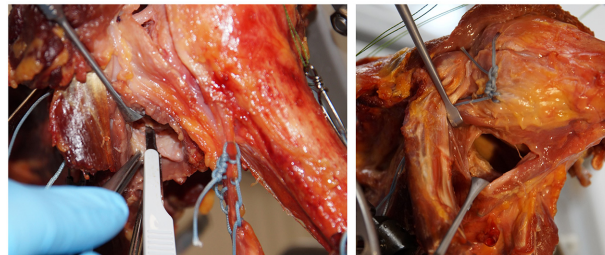


**Figure 1.** Preparation of human specimen. A labral lesion is applied via an anteroinferior capsulotomy.

were all preserved. To be capable of loading the delta muscle and the rotator cuff tendons, sutures were applied in Krakow stitch technique to each tendon, adjacent to the tendon's insertion points, with FiberWire Sutures (US 5, Arthrex). Hereafter, an anteroinferior capsule incision was performed to relieve negative intra-articular pressure and avoid influence of the vacuum effect on shoulder stability.<sup>5,8,9</sup>

To define joint-specific coordinate systems, 5 drill holes, each 2.7 mm in diameter, were placed into the cortical bone of the scapula and the proximal humerus. Using a CT scan, the drill holes and anatomic reference points were measured, resulting in a rigid body system for each bone. This spatial relationship was later used to calculate the position of anatomic reference points, such as the center of glenohumeral rotation or the humeral epicondyles, by measuring the fiducial points (drill holes) only.<sup>13,24,30</sup>

The specimens were then attached to a custom-made construction via Schanz screws and a ring fixator, allowing for individual, selective muscle loading. Four Schanz screws were drilled through the scapular spine as well as the medial and lateral scapular margins, to achieve maximum stability of the scapula in the test setup. The distal humerus was embedded in polyurethane casting resin (Ren-Cast PU, Gößl + Pfaff GmbH).

Since stability testing was performed in intact joints as well as in the presence of labral Bankart lesions and Bankart fractures, surgical modification of the specimens' glenoids was performed successively to allow each of the following testing stages (Figure 1)<sup>1,20</sup>: (1) intact glenohumeral joint, (2) labral detachment (Bankart lesion), (3) 10% GBL, and (4) 20% GBL.

These procedures were performed by an experienced, fellowship-trained shoulder surgeon via an anteroinferior capsulotomy (J.C.K.). Biomechanical testing was performed for each defect stage.

\*Address correspondence to Sebastian Oenning, MD, Department of Trauma, Hand and Reconstructive Surgery, University Hospital Muenster, Waldeyer Straße 1, Muenster, 48149, Germany (email: Sebastian.oenning@ukmuenster.de).

<sup>†</sup>Department of Trauma, Hand and Reconstructive Surgery, University Hospital Muenster, Muenster, Germany.

<sup>‡</sup>Faculty of Engineering Physics, FH Muenster, Muenster, Germany.

Final revision submitted November 7, 2023; accepted November 21, 2023.

The authors have declared that there are no conflicts of interest in the authorship and publication of this contribution. AOSSM checks author disclosures against the Open Payments Database (OPD). AOSSM has not conducted an independent investigation on the OPD and disclaims any liability or responsibility relating thereto.

Ethical approval for this study was obtained from the Ärztekammer Westfalen-Lippe and the University of Muenster (ref No. 2022-323-f-S).



**Figure 2.** Human specimen in robotic test setup with the distal humerus attached to a 6-axis industrial robot (KR 60-3, KUKA). Stable scapular fixation via Schanz screws and ring fixator. Loading of rotator cuff and deltoid muscle tendons with custom-made FiberWire-construction (US 5, Arthrex) in Krakow suture technique.

### Test Setup

To perform controlled glenohumeral translation, the scapula was fixed in a ring fixator, as described above, while the distal humerus was attached to a 6-axis industrial robot (KR 60-3, KUKA) (Figure 2). Its accuracy of position repeatability was  $\pm 60 \mu\text{m}$ . Forces arising during humeral motion were monitored by a force/torque sensor (FT Mini45, ATI Industrial Automation), which had a measurement error of  $\leq 0.25 \text{ N}$  and  $\leq 0.01 \text{ N}\cdot\text{m}$ , respectively. Robot control was performed with the simVITRO software (Cleveland Clinic BioRobotics Lab).

The scapular and humeral fiducial points (drill holes) were digitized using a 3D measuring arm (Absolute Arm 8320-7, Hexagon Metrology GmbH) with a measurement error of  $\leq 50 \mu\text{m}$ . In combination with the specimens' CT scans, a joint-specific 3D coordinate system was calculated using the rigid body definitions. To ensure specific glenohumeral translation, an individual coordinate system was defined for each specimen. Its mediolateral axis was directed from the scapular spine's medial border to the center of the humeral head. The anteroposterior axis was set orthogonally to the plane defined by the inferior angle, the scapular spine's medial border and the center of the humeral head. The superoinferior axis was then aligned orthogonally to the mediolateral and anteroposterior axes.

### Biomechanical Experiments

Load and shift testing was performed with the specimen fixed in  $60^\circ$  of glenohumeral abduction (corresponding to  $90^\circ$  of humerothoracic elevation) in neutral rotation, simulating an articular position with loosened capsule and

ligaments, in which stability is provided mostly by the glenoid shape and muscular guidance.<sup>10,15,16</sup>

To achieve centering of the humeral head and assess the anatomic stating position, an isolated compression force of  $10 \text{ N}$  was applied to the humerus first, while all other joint forces were minimized and no muscular loads were applied. To assess glenoid depth and concavity, the humeral head was shifted anteriorly to 90% of the anteroposterior glenoid radius and posteriorly to 50% of the glenoid radius at a maximum displacement rate of  $1 \text{ mm/s}$ . Since the humeral head hereby had continuous contact to the glenoid surface, the deepest point of the glenoid cavity was detected reliably.

Loading of the deltoid and rotator cuff tendons was then established. Due to the individual anatomy and different-sided specimens, the tension vectors were adapted by adjusting the construction for each specimen. Anatomic force application and muscle loading was then achieved. According to the muscular cross-sectional area and the physiological force ratio distributed by the rotator cuff and the deltoid muscle, the tendons were loaded to the following extent: the deltoid muscle was loaded with  $42.3 \text{ N}$  ( $14.1 \text{ N}$  for each of the 3 deltoid parts), the supraspinatus muscle (SSP) with  $8.7 \text{ N}$ , the infraspinatus (ISP) and teres minor muscle (TM) combined with  $22 \text{ N}$ , and the subscapularis muscle (SSC) with  $22.4 \text{ N}$ . After muscle loading, no further external compression forces were required for humeral head centering.<sup>7,25,31</sup>

To evaluate anteroinferior shoulder stability under muscle loading, the humeral head was again shifted anteriorly and posteriorly up to 90% and 50% of the glenoid radius, respectively, by the robot. Importantly, the robot performed position-controlled anteroposterior translation. Superoinferior and mediolateral shifting were not constrained and, therefore, force controlled. Thus, a physiological anteroinferior humeral translation was evoked, due to the humeral head seeking the path of least resistance and being deflected inferiorly by the coracoid. Nonconstrained mediolateral humeral motion was influenced by rotator cuff loading and the individual glenoid concavity. The anteriorly directed forces exerted by the robot to achieve a  $5 \text{ mm}$  anterior translation were monitored. This setup was repeated throughout the different testing stages, beginning with intact glenohumeral joints followed by equivalent testing in the presence of a labral Bankart lesion as well as Bankart fractures with 10% and 20% anteroinferior GBL, respectively.

Throughout all testing stages and specimens, the maximum force required for  $5 \text{ mm}$  of anterior translation under muscle loading and the direction of dislocation ( $0^\circ$  for anterior,  $>0^\circ$  for anterosuperior, and  $<0^\circ$  for anteroinferior dislocation) was measured. The initial glenoid depth and concavity were assessed by load and shift testing without muscle loading as well as by CT scans. In the robotic test setup, the glenoid depth was defined as the maximum lateral displacement of the humeral head during translation. The glenoid concavity was determined as the ratio of maximum lateral displacement in relation to the anterior displacement. In the CT scans, the BSSR was calculated using glenoid radius and depth.

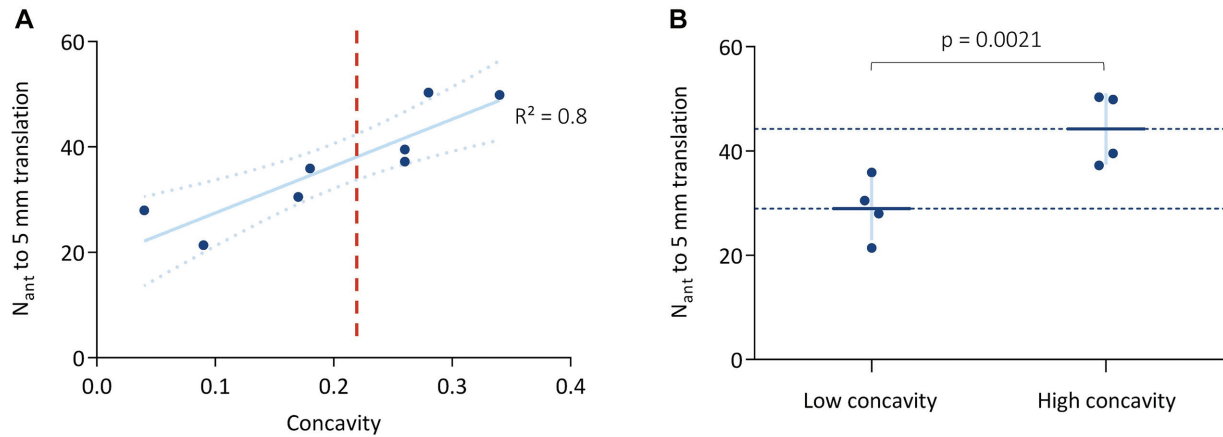


**Figure 3.** (A) Correlation between glenoid concavity and  $N_{ant}$  in a linear regression model with a determination coefficient of  $R^2 = 0.8$ . (B) Definition of LC and HC subgroups with significantly higher  $N_{ant}$  values in the HC subgroup in native specimens ( $P = .0021$ ). HC, high concavity; LC, low concavity;  $N_{ant}$ , anteriorly directed force to achieve a 5 mm anterior translation.

For subgroup analyses, 2 cohorts were defined. After an initial analysis of glenoid concavity, the 8 specimens were divided into 2 subgroups of 4 specimens each. Due to the unknown physiological ranges of glenoid concavity, the 4 specimens with the lowest concavity and the 4 specimens with the highest concavity were grouped together. Thus, 2 equally sized subgroups were formed, according to the specimens' concavity.

### Statistical Analysis

A custom-made MATLAB-script (R2019a, The MathWorks Inc) was developed for signal processing. Statistical analysis of the influence of each stage of glenoid pathology on shoulder stability was performed with GraphPad Prism Version 9 (GraphPad Software). For group comparisons, 2-way repeated-measures analysis of variance and Sidak post hoc test with a correction for multiple comparisons were chosen. A significance level of  $P < .05$  was set.

To analyze the correlation between maximum anterior force and glenoid depth and concavity, a linear regression model was applied, and the determination coefficient ( $R^2$ ) was used to measure the correlation.

## RESULTS

In the 8 native joints, a high correlation between glenoid concavity and the required anteriorly directed force to achieve a 5 mm anterior translation ( $N_{ant}$ ) was observed in a linear regression model with a determination coefficient of  $R^2 = 0.8$  (Figure 3A). The concavity values ranged from 0.19 to 2.19 and were divided into low concavity (LC) and high concavity (HC) subgroups. Concavity in these subgroups ranged from 0.19 to 1.31 and 1.89 to 2.19, respectively. Comparing the LC and HC subgroups, significantly

higher initial  $N_{ant}$  values were observed in the HC subgroup ( $P = .0021$ ; 95% CI, 5.021-25.57) (Figure 3B).

A difference between the LC and HC subgroups was also observed in the first stages of defect size, including labral Bankart lesions and a 10% anteroinferior bony glenoid defect. Significantly higher  $N_{ant}$  values were found in HC specimens compared with LC specimens ( $P = .0044$  and  $P = .0142$ , respectively). In the final defect size of 20% GBL, the mean  $N_{ant}$  was still higher in the HC subgroup compared with the LC subgroup, without showing statistical significance ( $P = .0621$ ) (Figure 4 and Table 1). In addition, mean  $N_{ant}$  in HC joints after applying a 20% glenoid lesion was higher than every mean  $N_{ant}$  value of the preceding testing stages in the LC subgroup without statistical significance.

Analyzing the  $N_{ant}$  values in each subgroup, a significant decrease of  $N_{ant}$  was found in the HC subgroup in every defect stage compared with the native  $N_{ant}$  values (Bankart lesion:  $P = .0104$ , 10% GBL:  $P = .0002$ , 20% GBL:  $P < .0001$ ). The decrease in stability between labral lesions and 10% bony defect was not statistically significant ( $P = .4014$ ; 95% CI, -1.04 to 4.48), whereas the transition from 10% to 20% GBL led to significantly lower  $N_{ant}$  values ( $P = .0118$ ; 95% CI, 0.62 to 6.14). In the LC subgroup, significantly reduced  $N_{ant}$  values were observed in the 20% bony defect stage compared with the native testing stage ( $P = .0206$ ; 95% CI, 0.38 to 5.91).

Regarding the loss of anterior shoulder stability, it was observed that bony defects led to a higher reduction of  $N_{ant}$  in specimens with an initial HC. There was no significant difference in loss of  $N_{ant}$  between both subgroups after applying labral lesions ( $P = .8269$ ; 95% CI, -2.96 to 4.97). However, we found a significantly higher loss of  $N_{ant}$  in the 20% bony defect stage in the HC subgroup compared with the LC subgroup ( $P = .0049$ ; 95% CI, 1.56 to 9.22) (Figure 5). In a linear regression model analyzing the loss of  $N_{ant}$  in the 20% bony defect stage, we found a high determination coefficient of  $R^2 = 0.86$ . The high correlation

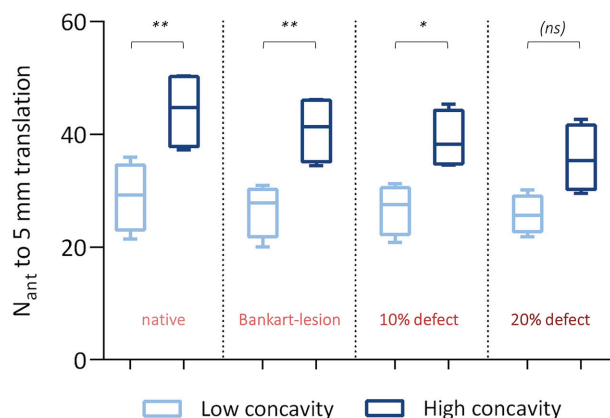


**Figure 4.**  $N_{ant}$  values of LC and HC subgroups throughout all testing stages. Significantly higher  $N_{ant}$  values were seen in the HC subgroup in native joints and after applying Bankart lesions and 10% bony glenoid defects ( $P < .05$ ). There was no statistical significance (ns) at the 20% bony defect stage ( $P = .0621$ ). HC, high concavity; LC, low concavity;  $N_{ant}$ , anteriorly directed force to 5 mm anterior translation. Statistically significant differences are indicated (\*,  $P < .05$ ; \*\*,  $P < .01$ ).

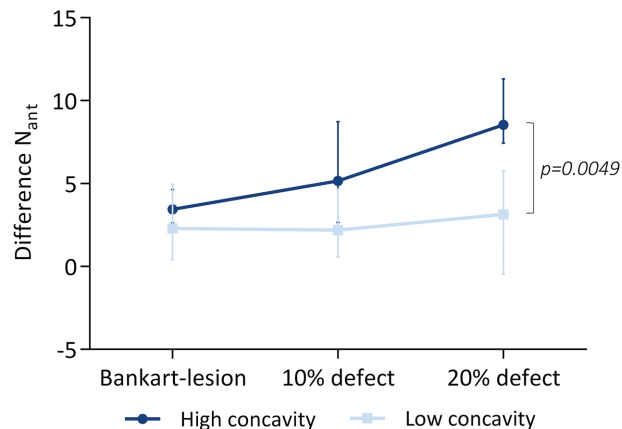


**Figure 5.** Mean loss of  $N_{ant}$  values in the LC and HC subgroups throughout all testing stages compared with  $N_{ant}$  values in native joints. A significantly higher loss of  $N_{ant}$  in the HC subgroup was seen compared to LC joints in 20% bony defect stage ( $P = .0049$ ). HC, high concavity; LC, low concavity;  $N_{ant}$ , anteriorly directed force to 5 mm anterior translation.

indicates that the more initial concavity was present in the specimens, the more they suffered from stability loss in 20% glenoid defects (Figure 6).

In addition, the correlation of the specimens' CT-based BSSR with their  $N_{ant}$  and loss of  $N_{ant}$  was assessed. Throughout all testing stages from native joints to 20% bony defects, a medium-to-good correlation between BSSR and anterior shoulder stability was found. For example, the determination coefficient in a linear regression model for the correlation between  $N_{ant}$  in native joints and the CT-based BSSR was  $R^2 = 0.52$ . Statistical analyses showed comparable values for the loss of  $N_{ant}$  after applying Bankart lesions and 10% and 20% bony glenoid defects ( $R^2 = 0.56, 0.59, \text{ and } 0.49$ , respectively).

## DISCUSSION

In this biomechanical model including soft tissue and the rotator cuff's concavity compression, we can summarize the following main findings: (1) the glenoid concavity showed a high correlation with anterior shoulder stability. High glenoid concavity led to a high glenohumeral stability, thus playing a major role in preventing anteroinferior dislocation of the humeral head. (2) In labral and bony glenoid defects, highly concave-shaped glenoids lose more stability than glenoids with initial LC. However, even with 20% GBL, the HC subgroup provided higher absolute stability values than native, intact LC glenoids. Since this difference was not statistically significant, we assume that the small sample size of 8 specimens was not sufficient to create significant results. Nevertheless, it underlines the importance of glenoid concavity for shoulder stability.

Understanding global glenohumeral stability as the summation of bony stability and other soft tissue-related

stabilizing factors, the glenoid concavity can be considered decisively responsible for bony stability. In glenohumeral joints with low glenoid concavity, stability would have to be achieved by other stabilizing factors (higher, compressive forces exerted by the rotator cuff, for example) to withstand anterior dislocation force. The impact of the glenoid retroversion angle on bony glenohumeral stability is not yet known.

Threshold values indicating bony reconstruction have long been a matter of discussion. Recent studies have revealed a relevant increase of instability in glenoid defects between 13.5% and 16%.<sup>3,12,21,22</sup> In previous literature, the range of subcritical GBL differs between 13.5% and 25%.<sup>21,22,32</sup> Our results lead us to consider the loss of glenoid concavity to be a more precise predictor for persistent glenohumeral instability compared with size of a glenoid defect. Especially in patients with subcritical bone loss, the loss of concavity can help to assess the need for bony glenoid reconstruction. Thus, the initial glenoid concavity, as well as the loss of concavity, should be considered as part of an individual, therapeutic approach. For future studies, the unknown impact of additional stabilizing factors (glenoid retroversion, muscular forces, and capsular tension, for example) should be considered. This leads to the question of whether surgical treatment should focus on reconstructing the initial concavity or building up a higher concavity to increase bony stability.

Regarding the CT-based BSSR, we found a medium-to-good correlation between the BSSR and anterior glenohumeral stability and the loss of stability in our specimens. We consider this to be due mainly to the rather small sample size of 8 and would expect the correlation to be higher in future studies including a larger number of specimens. Also, the individual chondral morphology and integrity could cause differences between the BSSR and the glenohumeral

TABLE 1  
Anteriorly Directed Force to 5 mm Anterior Translation<sup>a</sup>

	Native	Bankart Lesion	10% GBL	20% GBL
LC	28.95	26.65	26.76	25.8
HC	44.24	40.81	39.09	35.71
<i>P</i> value (LC vs HC)	.0021 (**)	.0044 (**)	.0142 (*)	.0621 (ns)
95% CI	5.02 to 25.57	3.881 to 24.43	2.05 to 22.6	-0.37 to 20.18

<sup>a</sup>Data are reported as mean unless otherwise indicated. Statistical analysis of  $N_{ant}$  in all testing stages, including comparison of LC and HC subgroups for each testing stage by 2-way analysis of variance and Sidak post hoc test with correction for multiple comparisons. GBL, glenoid bone loss; HC, high concavity; LC, low concavity;  $N_{ant}$ , anteriorly directed force to 5 mm anterior translation; Statistically significant differences are indicated (\*,  $P < .05$ ; \*\*,  $P < .01$ ); ns, not significant.

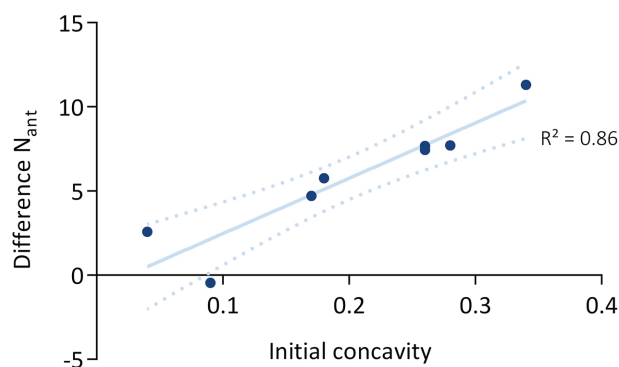


**Figure 6.** Linear regression model of the loss of  $N_{ant}$  and initial glenoid concavity in 20% bony glenoid defect testing stage. The high determination coefficient of  $R^2 = 0.86$  indicates greater correlation between glenoid concavity and loss of anterior glenohumeral stability.  $N_{ant}$ , anteriorly directed force to 5 mm anterior translation.

stability in our biomechanical model. Since the BSSR is based on CT scans, chondral and labral effects on glenohumeral stability were not taken into account.<sup>14,17,28</sup>

### Limitations

Regarding our biomechanical model, the rather small number of specimens can be considered a limitation, although it lies within the range of sample sizes in comparable, cadaveric studies.<sup>5,29</sup> We assumed that our results within the 20% GBL testing stage and the correlation between measured concavity and BSSR would be clearer in case of larger sample sizes. However, all shoulder joints and their soft tissue surroundings were examined and ruled out in case of preexisting, macroscopic injury, resulting in 8 specimens for biomechanical testing. Exclusion was performed by macroscopic inspection, as well as CT and magnetic resonance imaging scans of all potential specimens. Rotator cuff tears, chondral lesions, and osteophytes could be detected reliably, which led to excluding specimens. We sought to increase our study's quality and reliability as a result.

Due to the specimens' older age, with a mean of  $82.3 \pm 8.12$  years, microscopic, degenerative changes could still

have affected shoulder stability and tendon integrity. Thus, muscle loading was applied carefully to prevent tendon rupture, as Williamson et al<sup>29</sup> described SSP tendon tears in the case of loading  $>20$  N. In addition, the same muscle loading protocol was applied to all specimens, not adjusting it to the individual donor's size and weight. In previous literature, testing protocols varied from static to partially and fully dynamic muscle loading. Since we performed testing with the specimen fixed in  $60^\circ$  of glenohumeral abduction, differentiated, static loading protocols were used. Wu et al<sup>31</sup> described the force distribution of various muscles involved in glenohumeral motion. The ratio of deltoid and rotator cuff force exertion during active glenohumeral abduction to  $60^\circ$  was comparable with the ratio of the muscles' anatomic cross-section areas.<sup>25,31</sup> Therefore, it was implemented in our model to achieve physiological conditions, while the scale of loading forces was similar to that of recent cadaveric studies.<sup>5,29</sup> However, it remains probable that the physiological compression force exerted by the rotator cuff exceeds that of our muscle loading protocol, as Klemm et al<sup>11</sup> pointed out in their study regarding daily life, shoulder-related activity.

Finally, it is unknown whether our subgroup determination is consistent with the physiological range of glenoid concavity. In this study, the group of 8 specimens was divided into 2 equally sized subgroups according to their concavity, due to the unknown physiological ranges of concavity.

Further biomechanical and clinical studies are needed to establish reference values and develop therapeutic algorithms. The evaluation of physiological glenoid concavity and retroversion as well as its clinical relevance are our working group's current and future study topics.

### CONCLUSION


Glenoid concavity is an essential factor for anterior glenohumeral stability in an active-assisted, biomechanical model including soft tissue surroundings. High concave-shaped glenoids – even in the presence of GBL – showed a higher stability than intact shoulder joints with LC. Therefore, in the case of posttraumatic or chronic anterior shoulder instability, the glenoid concavity must be considered. The results of this study should be translated into

a clinical setting to allow an individual, therapeutic approach considering glenoid concavity as an important factor for glenohumeral stability.

## ACKNOWLEDGMENTS

We acknowledge support by the Open Access Publication Fund of University of Muenster. There was no additional external funding received for this study. The funders had no role in study design, data collection and analysis, decision to publish, or preparation of the manuscript.

## ORCID iD

Sebastian Oenning  <https://orcid.org/0009-0004-2022-0569>

## REFERENCES

- Bockmann B, Venjakob AJ, Reichwein F, Hagenacker M, Nebelung W. Mapping of glenoid bone loss in recurrent anterior shoulder instability: is there a particular deficit pattern? *J Shoulder Elbow Surg.* 2017;26(9):1676-1680.
- Burkhart SS, De Beer JF. Traumatic glenohumeral bone defects and their relationship to failure of arthroscopic Bankart repairs: significance of the inverted-pear glenoid and the humeral engaging Hill-Sachs lesion. *Arthroscopy.* 2000;16(7):677-694.
- Dickens JF, Owens BD, Cameron KL, et al. The effect of subcritical bone loss and exposure on recurrent instability after arthroscopic Bankart repair in intercollegiate American football. *Am J Sports Med.* 2017;45(8):1769-1775.
- Dickens JF, Slaven SE, Cameron KL, et al. Prospective evaluation of glenoid bone loss after first-time and recurrent anterior glenohumeral instability events. *Am J Sports Med.* 2019;47(5):1082-1089.
- Dyrna F, Kumar NS, Obopilwe E, et al. Relationship between deltoid and rotator cuff muscles during dynamic shoulder abduction: a biomechanical study of rotator cuff tear progression. *Am J Sports Med.* 2018;46(8):1919-1926.
- Griffith JF, Antonio GE, Yung PSH, et al. Prevalence, pattern, and spectrum of glenoid bone loss in anterior shoulder dislocation: CT analysis of 218 patients. *AJR Am J Roentgenol.* 2008;190(5):1247-1254.
- Halder AM, O'Driscoll SW, Heers G, et al. Biomechanical comparison of effects of supraspinatus tendon detachments, tendon defects, and muscle retractions. *J Bone Joint Surg Am.* 2002;84(5):780-785.
- Hirschler C, Wülker N, Mendila M. The effect of negative intraarticular pressure and rotator cuff force on glenohumeral translation during simulated active elevation. *Clin Biomech (Bristol, Avon).* 2000;15(5):306-314.
- Ishihara Y, Mihata T, Tamboli M, et al. Role of the superior shoulder capsule in passive stability of the glenohumeral joint. *J Shoulder Elbow Surg.* 2014;23(5):642-648.
- Itoi E, Lee SB, Berglund LJ, Berge LL, An KN. The effect of a glenoid defect on antero-inferior stability of the shoulder after Bankart repair: a cadaveric study. *J Bone Joint Surg Am.* 2000;82(1):35-46.
- Klemt C, Prinold JA, Morgans S, et al. Analysis of shoulder compressive and shear forces during functional activities of daily life. *Clin Biomech (Bristol, Avon).* 2018;54:34-41.
- Klemt C, Toderita D, Nolte D, Di Federico E, Reilly P, Bull AMJ. The critical size of a defect in the glenoid causing anterior instability of the shoulder after a Bankart repair, under physiological joint loading. *Bone Joint J.* 2019;101-B(1):68-74.
- Kolz CW, Sulkar HJ, Aliaj K, et al. Reliable interpretation of scapular kinematics depends on coordinate system definition. *Gait Posture.* 2020;81:183-190.
- Lazarus MD, Sidles JA, Harryman DT II, Matsen FA III. Effect of a chondral-labral defect on glenoid concavity and glenohumeral stability: a cadaveric model. *J Bone Joint Surg Am.* 1996;78(1):94-102.
- Lippitt SB, Vanderhooft JE, Harris SL, Sidles JA, Harryman DT II, Matsen FA III. Glenohumeral stability from concavity-compression: a quantitative analysis. *J Shoulder Elbow Surg.* 1993;2(1):27-35.
- Ludewig PM, Phadke V, Braman JP, Hassett DR, Cieminski CJ, LaPrade RF. Motion of the shoulder complex during multiplanar humeral elevation. *J Bone Joint Surg Am.* 2009;91(2):378-389.
- Lugo R, Kung P, Ma CB. Shoulder biomechanics. *Eur J Radiol.* 2008;68(1):16-24.
- Moroder P, Damm P, Wierer G, et al. Challenging the current concept of critical glenoid bone loss in shoulder instability: does the size measurement really tell it all? *Am J Sports Med.* 2019;47(3):688-694.
- Moroder P, Ernstbrunner L, Pomwenger W, et al. Anterior shoulder instability is associated with an underlying deficiency of the bony glenoid concavity. *Arthroscopy.* 2015;31(7):1223-1231.
- Saito H, Itoi E, Sugaya H, Minagawa H, Yamamoto N, Tuoheti Y. Location of the glenoid defect in shoulders with recurrent anterior dislocation. *Am J Sports Med.* 2005;33(6):889-893.
- Shaha JS, Cook JB, Song DJ, et al. Redefining "critical" bone loss in shoulder instability. *Am J Sports Med.* 2015;43(7):1719-1725.
- Shin SJ, Ko YW, Scott J, McGarry MH, Lee TQ. The effect of defect orientation and size on glenohumeral instability: a biomechanical analysis. *Knee Surg Sports Traumatol Arthrosc.* 2016;24(2):533-539.
- Souleiman F, Zderic I, Pastor T, et al. Cartilage decisively shapes the glenoid concavity and contributes significantly to shoulder stability. *Knee Surg Sports Traumatol Arthrosc.* 2022;30(11):3626-3633.
- Sulkar HJ, Zitnay JL, Aliaj K, Henninger HB. Proximal humeral coordinate systems can predict humerothoracic and glenohumeral kinematics of a full bone system. *Gait Posture.* 2021;90:380-387.
- Veeger HEJ, Van Der Helm FCT, Van Der Woude LHV, Pronk GM, Rozendal RH. Inertia and muscle contraction parameters for musculoskeletal modelling of the shoulder mechanism. *J Biomech.* 1991;24(7):615-629.
- Wermers J, Raschke MJ, Wilken M, Riegel A, Christoph Katthagen J. The anatomy of glenoid concavity - bony and osteochondral assessment of a stability-related parameter. *J Clin Med.* 2021;10(19):4316.
- Wermers J, Schliemann B, Raschke MJ, et al. Glenoid concavity has a higher impact on shoulder stability than the size of a bony defect. *Knee Surg Sports Traumatol Arthrosc.* 2021;29(8):2631-2639.
- Wermers J, Schliemann B, Raschke MJ, et al. The glenolabral articular disruption lesion is a biomechanical risk factor for recurrent shoulder instability. *Arthrosc Sports Med Rehabil.* 2021;3(6):e1803-e1810.
- Williamson PM, Hanna P, Momenzadeh K, et al. Effect of rotator cuff muscle activation on glenohumeral kinematics: a cadaveric study. *J Biomech.* 2020;105(10):109798.
- Wu G, Van Der Helm FCT, Veeger HEJ, et al. ISB recommendation on definitions of joint coordinate systems of various joints for the reporting of human joint motion - Part II: shoulder, elbow, wrist and hand. *J Biomech.* 2005;38(5):981-992.
- Wu W, Lee PVS, Bryant AL, Galea M, Ackland DC. Subject-specific musculoskeletal modeling in the evaluation of shoulder muscle and joint function. *J Biomech.* 2016;49(15):3626-3634.
- Yamamoto N, Kawakami J, Hatta T, Itoi E. Effect of subcritical glenoid bone loss on activities of daily living in patients with anterior shoulder instability. *Orthop Traumatol Surg Res.* 2019;105(8):1467-1470.